CHARLES H. LANGE and DONALD D. DUNCAN

TEMPERATURE COEFFICIENTS OF THE REFRACTIVE INDEX FOR CANDIDATE OPTICAL WINDOWS

The temperature coefficients of the refractive index for various crystalline and polycrystalline materials—Al_2O_3 (sapphire), Y_2O_3 (yttria), La_2O_3-doped Y_2O_3, $MgAl_2O_4$, and ALON (a proprietary ceramic composed of aluminum, oxygen, and nitrogen)—were determined from measurements of optical thickness as a function of temperature using a Michelson interferometer operating at 0.633 μm. For temperatures between 23 and 500°C, the first-order coefficients ranged from 8.3×10^{-6}/°C for pure yttria to 14.6×10^{-6}/°C for ALON. Measurements of NaCl and Al_2O_3 samples using this technique are in agreement with published data.

INTRODUCTION

Optical systems often require a protective window, called a sensor dome, to guard against extreme heat and temperature and pressure gradients. The refractive nature of any sensor dome material requires that the window be viewed as an integral part of the imaging system. Because the windows can degrade the image quality, especially under adverse conditions, characterization of the refractive nature of sensor dome materials is required. Knowledge of the temperature dependence of the refractive index is necessary for a complete evaluation of the dome's optical performance. To assess their potential for use as IR sensor windows, the temperature coefficients of the refractive index (dn/dT) of various crystalline and polycrystalline materials—Al_2O_3 (ordinary ray), Y_2O_3, La_2O_3-doped Y_2O_3, $MgAl_2O_4$, and ALON—were determined at 0.633 μm.

The refractive index is typically determined by using a glass prism composed of the desired material.[1] Although measuring the minimum ray deviation for a specific wavelength is extremely accurate, it has the disadvantage of requiring specific sample geometries and does not lend itself to measurement of samples that are highly scattering. The technique for measuring optical thickness described in this article only requires knowledge of sample thickness and is accurate for samples that are highly scattering.

Thermal coefficients of the refractive index measured at 0.633 μm can be used to estimate the high-frequency permittivity $\epsilon_\infty(T)$ in a temperature-dependent phenomenological pole fit model.[2] This model can then be used to predict refractive index as a function of wavelength and temperature.

MATHEMATICAL MODEL

The optical thickness (which differs from the physical thickness) of the windows was measured as a function of temperature using the experimental configuration shown in Figure 1. Measurements were made using a Hewlett-Packard 5501A Michelson interferometer operating at 0.633 μm. This device measures the phase shift between the reference and measurement beams and

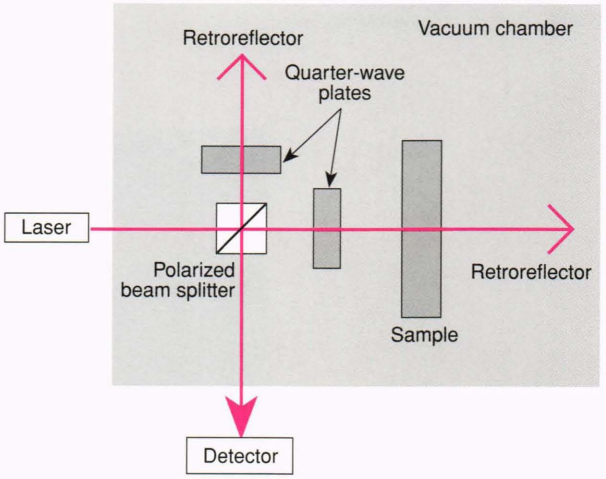

Figure 1. Schematic of experimental configuration.

counts every $\lambda/2$ increase in optical path (a change of $\lambda/4$ in the optical path of the measurement arm). Samples of various materials were placed in a temperature-controlled hot cell that was then placed within the measurement beam of the interferometer. The interferometer was mounted on an Invar plate inside a vacuum chamber. Invar was used because of its low coefficient of thermal expansion. This plate eliminated warpage and expansion problems, which can introduce error into the measurements. The vacuum chamber eliminated fluctuations in the optical path caused by barometric pressure fluctuations and aided in temperature control of the interferometer components and the sample.

Figure 2 shows the path lengths involved in the experiment. For a single pass, the optical path length (OPL) of the sample arm of the interferometer is given by

$$\mathrm{OPL} = (L_1 + L_2) + wn\,, \qquad (1)$$

where L_1 and L_2 are the portions of the path length in the vacuum, w is the thickness of the sample, and n is its refractive index. A quadratic model was assumed for the thickness as a function of temperature, expressed as

$$w = w_0(1 + \alpha_1 T + \alpha_2 T^2), \tag{2}$$

and for the refractive index,

$$n = a_0 + a_1 T + a_2 T^2, \tag{3}$$

where α_1 and α_2 are the linear and quadratic coefficients of expansion expressed as a function of temperature; a_0, a_1, and a_2 are the refractive index and its linear and quadratic coefficients, respectively; and T is temperature. The derivative of the OPL with respect to temperature is obtained from Equation 1 by

$$\frac{d\text{OPL}}{dT} = \frac{\partial L}{\partial T} + n\frac{\partial w}{\partial T} + w\frac{\partial n}{\partial T}, \tag{4}$$

where L is the sum of L_1 and L_2.

The partial derivatives with respect to the temperature are from Equations 2 and 3 as follows:

$$\frac{\partial w}{\partial T} = w_0(\alpha_1 + 2\alpha_2 T), \tag{5}$$

$$\frac{\partial n}{\partial T} = a_1 + 2a_2 T. \tag{6}$$

From Figure 2, we note that

$$\frac{\partial L}{\partial T} = -\frac{\partial w}{\partial T}. \tag{7}$$

A second-order polynomial was fit by least-squares error to the experimental optical path length data. The derivative of this fit with respect to temperature is given by

$$\frac{d\text{OPL}}{dT} = b_1 + 2b_2 T, \tag{8}$$

where b_1 and b_2 are experimentally determined numbers. From Equations 4 through 8 and equating like powers of temperature, we obtain the following relationships between the desired coefficients and the experimentally determined coefficients:

$$a_1 = \frac{b_1}{w_0} + \alpha_1(1 - a_0), \tag{9a}$$

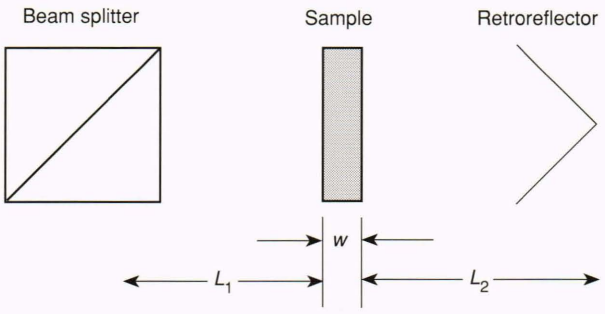

Figure 2. Diagram of path length calculations.

$$a_2 = \frac{b_2}{w_0} + \alpha_2(1 - a_0) - \alpha_1 a_1, \tag{9b}$$

where

$$a_0 = n(T_0), \qquad w_0 = w(T_0). \tag{9c}$$

The experiment was designed to determine the coefficients b_1 and b_2. The analysis relied upon various references for the refractive index $n(T_0)$ and the coefficients of thermal expansion α_1 and α_2. Equations 9a, 9b, and 9c are the results of these calculations.

RESULTS

Calculation of the refractive index of the thermal coefficients required knowledge of the sample's temperature. Since the thermocouple was located near the edge of the sample and OPL was measured at the center of the sample, the experiment required that the temperature be uniform throughout the sample. The experiment took roughly two days; a two-hour stabilization interval for each temperature step ensured a uniform sample temperature. To provide continuous data, measurements were taken every minute to determine whether the sample was reaching a stable temperature. The temperature was raised and lowered during the course of each experiment to detect any variations in the sample temperature measurements with data taken during each phase. Figure 3 shows a plot of the temperature history for sapphire during the measurement period. The "hysteresis" appears because the sample temperature lagged behind the temperature recorded by the thermocouple. Figure 4 is the temperature-dependent OPL for NaCl; the data were taken after the temperature had stabilized, that is, when the temperature was uniform across the sample.

A quadratic curve was fit to the data corresponding to the stable temperature points. The first-order term reveals the temperature variation of the optical path from which dn/dT can be derived. A quadratic fit was used to obtain a more accurate coefficient for the first-order term. Typ-

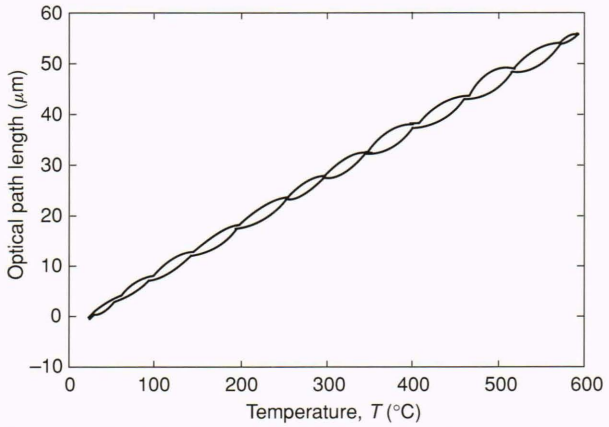

Figure 3. Typical temperature history of a sapphire sample over a 54-hour measurement period at a wavelength of 0.633 μm. Sample thickness was 0.25 in. The convex upward portion of the curve is the path taken on the heating cycle; the concave upward portion is the cooling cycle.

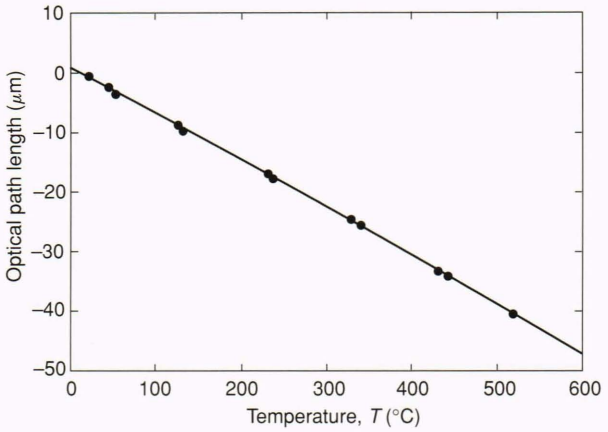

Figure 4. Optical path length (OPL) data and quadratic fit for NaCl measured at a wavelength of 0.633 μm. (OPL = 0.837 − 0.0761T − 6.96 × $10^{-6}T^2$.) The sample thickness was 0.204 in.

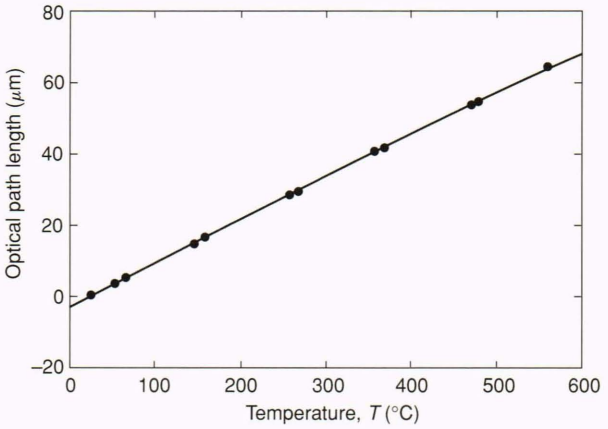

Figure 5. Optical path length (OPL) data and quadratic fit for ALON measured at a wavelength of 0.633 μm. (OPL = −2.26 + 0.121T − 7.80 × $10^{-6}T^2$.) The sample thickness was 0.25 in.

Table 1. Dimensions and thermal coefficients of expansion for various materials.

Material	Thickness, w_0 (in.)	Linear coefficient, α_1 ($°C^{-1}$) (× 10^{-6})	Quadratic coefficient, α_2 ($°C^{-2}$) (× 10^{-9})
NaCl[a]	0.204	44.0	—
NaCl[b]	—	39.7	—
$LiNbO_3$ (C-cut)[c]	0.070	4.1	—
Al_2O_3 (C-cut)[d]	0.250	6.18 ± 0.16	2.18 ± 0.19
Y_2O_3 (pure)[d]	0.250	6.38 ± 0.36	1.53 ± 0.37
La_2O_3-doped Y_2O_3[d]	0.234	6.72 ± 0.10	1.19 ± 0.10
$MgAl_2O_4$[d]	0.197	6.21 ± 0.50	3.03 ± 0.61
ALON[d]	0.250	5.63 ± 0.07	2.17 ± 0.07

Note: Dashes indicate that data are unavailable.
[a]Data from Ref. 3.
[b]Data from Ref. 4.
[c]Data from Ref. 5.
[d]Data from Ref. 6.

Table 2. Parameters of fit to optical path length data for various materials.

Material	Linear coefficient, b_1 (μm/°C)	Quadratic coefficient, b_2 (μm/$°C^2$) (× 10^{-6})
NaCl	-0.076136	-6.96
$LiNbO_3$ (C-cut)	0.022532	0.692
Al_2O_3 (C-cut)	0.10437	-10.9
Y_2O_3 (pure)	0.090067	-15.1
La_2O_3-doped Y_2O_3	0.085504	-17.1
$MgAl_2O_4$	0.086126	-9.75
ALON	0.12090	-7.80

ical data sets and the resulting fits are shown in Figures 4 and 5.

The thermal coefficients of expansion (α_1 and α_2) for the different materials are given in Table 1. Owing to the similarities among the last five materials, their linear coefficients all are within ±9% of the mean value of 6.22 × 10^{-6}/°C, as expected.

Data on the parameters of the fit to the measured OPL data are shown in Table 2, and the refractive indices and temperature coefficients of the refractive index are given in Table 3. Note that for the similar materials (the last five materials listed in each of the tables), the temperature coefficients of the refractive index vary more than do the thermal expansion coefficients.

It was assumed that the error in the estimate of the first-order coefficient a_1 could be expressed as the root-sum-square of the various error sources. With reference to Equation 9a, the error can be expressed as

$$\Delta a_1 = \{(\Delta b_1/w_0)^2 + (b_1\Delta w_0/{w_0}^2)^2 + [(1 - a_0)\Delta\alpha_1]^2 + (\alpha_1\Delta a_0)^2\}^{1/2} . \quad (10)$$

In Equation 10, the first term on the right represents error in the calculation of the linear term in the fit of the OPL data. Virtually no error occurs in the regression fit per se. The error that arises in the calculation of b_1 is caused, for the most part, by the uncertainty in the actual sample temperature. The error was assumed to be 2% of the actual reading from the thermocouple. If the temperature T is replaced with the augmented temperature $T + \Delta T$ in the calculation of the fit to the OPL data, then it is seen that $\Delta b_1 = 2b_2\Delta T$. Incidentally, this result explains the lack of error estimates for a_2; uncertainties in a given parameter of the OPL data (caused mainly by uncertainties in the temperature) are due to the values of the higher-order terms in the fit. The OPL data were fit only through second order.

The second error term in Equation 10 is caused by uncertainties in the sample thickness. This uncertainty was taken to be 0.001 in. The third error term is caused by uncertainty in the value of the linear coefficient of expansion, and the fourth error term is caused by uncertainty in the refractive index at room temperature.

Table 3. Temperature coefficients of the refractive index for various materials.

Material	Refractive index, a_0	Linear coefficient, $a_1(°C^{-1})$ ($\times 10^{-6}$)	Quadratic coefficient, $a_2(°C^{-2})$ ($\times 10^{-9}$)
NaCl	1.5310[a]	−38.1	—
		−35.8	—
$LiNbO_3$ (C-cut)	2.2320[a]	7.62	—
Al_2O_3 (C-cut)	1.7659[b]	11.7 ± 0.2	−0.0050
Y_2O_3 (pure)	1.9253[c]	8.3 ± 0.3	−0.0038
La_2O_3-doped Y_2O_3	1.8965[d]	8.4 ± 0.1	−0.0040
$MgAl_2O_4$	1.6837[d]	13.0 ± 0.4	−0.0036
ALON	1.7900[d]	14.6 ± 0.1	−0.0030

Note: Dashes indicate that data are unavailable.
[a]Data from Ref. 5.
[b]Data from Ref. 7.
[c]Data from Ref. 8.
[d]Based on interpretation of Sellmeir parameters from manufacturer's data.

Of all the error terms in Equation 10, the dominant term by far is that caused by uncertainty in the linear coefficient of thermal expansion. The errors for this parameter, indicated in Table 1, are the estimates of measurement precision reported by The Southern Research Institute.[6] The error estimates for the linear thermal coefficients of refractive index are dominated in turn by these estimates.

DISCUSSION AND CONCLUSIONS

The first-order temperature coefficients of the refractive index for candidate optical window materials—Al_2O_3 (ordinary ray), Y_2O_3, La_2O_3-doped Y_2O_3, $MgAl_2O_4$, and ALON–ranged from 8.3 $\times$ 10^{-6}/°C for pure yttria to 14.6 $\times$ 10^{-6}/°C for ALON. The coefficients were determined from measurements of the optical thickness as a function of temperature over the range 23 to 500°C using a Michelson interferometer operating at 0.633 μm in vacuum. To verify our experimental technique, the first-order temperature coefficients of NaCl and $LiNbO_3$ were also measured. Estimates of the coefficient for NaCl (−38.1 $\times$ 10^{-6}/°C or −35.8 $\times$ 10^{-6}/°C, depending on the assumed thermal expansion coefficient) determined from the experiment compared favorably with the value of −32 $\times$ 10^{-6}/°C quoted by Li[1] and the value of −34.2 $\times$ 10^{-6}/°C given in the *CRC Handbook of Laser Science and Technology*.[5] Results for sapphire (11.7 $\times$ 10^{-6}/°C) were consistent with those reported in the *CRC Handbook*:[5] 11.7 $\times$ 10^{-6}/°C at a wavelength of 0.4579 μm. The results for $LiNbO_3$ (7.62 $\times$ 10^{-6}/°C) differed somewhat from the value of 10.4 $\times$ 10^{-6}/°C reported by Boyd et al.[9]

REFERENCES

[1] Li, H. H., "Refractive Index of Alkali Halides and Its Wavelength and Temperature Derivatives," *J. Phys. Chem. Ref. Data* **5**, 330-332, 528 (1976).
[2] Born, M., and Huang, K., *Dynamical Theory of Crystal Lattices*, Oxford University Press, London, p. 121 (1956).
[3] Wolfe, W. L., and Zissis, G. J. (eds.), *The Infrared Handbook*, Environmental Research Institute of Michigan, Ann Arbor (1985).
[4] Gray, D. E. (ed.), *American Institute of Physics Handbook*, 3rd Ed., McGraw–Hill, New York (1972).
[5] Weger, M. J. (ed.), *CRC Handbook of Laser Science and Technology*, Volume IV, Optical Materials-Properties, Part 2, CRC Press, Inc., Boca Raton, Fla. (1988).
[6] Southern Research Institute, *Mechanical and Thermal Properties of Four IR Dome Materials*, Birmingham, Ala. (1988).
[7] Malitson, I. H., "Refraction and Dispersion of Synthetic Sapphire," *J.Opt. Soc. Am.* **52**, 1377-1379 (Dec 1962).
[8] Nigara, Y., "Measurements of the Optical Constants of Yttrium Oxide," *Jpn. J. Appl. Phys.* **7**, 404-408 (Apr 1968).
[9] Boyd, G. D., Bond, W. L., and Carter, H. L., "Refractive Index as a Function of Temperature in $LiNbO_3$," *J. Appl. Phys.* **38**, 1941-1943 (15 Mar 1967).

THE AUTHORS

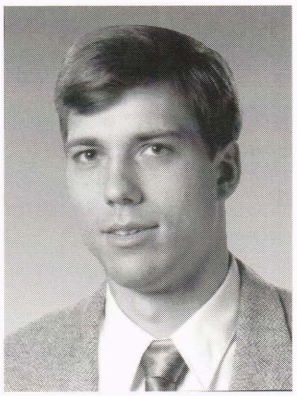

CHARLES H. LANGE is a member of APL's Associate Staff. He received his M.S. in electrical engineering from Texas A&M University in 1989, where his thesis work involved measurement, using optical modulation, of the intrinsic frequency response of semiconductor lasers. Since joining APL, he has worked on the characterization of polycrystalline materials, including bulk scatter properties and the dependence of refractive index on temperature. He has been involved with the alignment and characterization of an IR missile test facility whose purpose is to evaluate the dynamic tracking characteristics of missile seekers. Mr. Lange is currently the principal investigator on an independent research and development project aimed at developing infrared spatial light modulators using vanadium dioxide, and he also is the lead engineer for a set of space-borne imaging spectrographs.

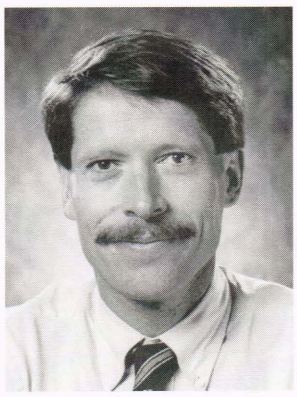

DONALD D. DUNCAN is supervisor of the Measurements and Propagation Section of APL's Electro-Optical Systems Group. He received his Ph.D. in electrical engineering from The Ohio State University in 1977. From 1977 to 1983, he was employed by Pacific-Sierra Research Corporation, where he modeled optical propagation phenomena such as aerosol scatter, atmospheric turbulence, and high-energy laser effects (e.g. thermal blooming, aerosol burnoff). Since joining APL in 1983, Dr. Duncan has worked on various biomedical engineering projects; provided test program support and data analysis for a tracking/guidance synthetic aperture radar system; and worked on many measurement, modeling, and diagnostic equipment projects in support of the hypersonic interceptor. He also teaches courses in Fourier and statistical optics at The Johns Hopkins University G.W.C. Whiting School of Engineering.